DESIGN AND CONTROL OF A SENSOR-GUIDED NANOROBOT

Markus Brunner and Andreas Stemmer

Institute of Robotics, Nanotechnology Group
Swiss Federal Institute of Technology Zurich (ETHZ)

ABSTRACT

Miniaturization is a key step in the design of integrated circuits. Intelligent systems working on the micro- and nanometer scale, i. e. "nanorobots", would be of great value in this miniaturization phase. They would help optimizing the design and production process by acquiring local sample information and they even might work as nanotools to fix tiny imperfections. To create such a nanorobot we extended the capabilities of an atomic force microscope (AFM) beyond the standard surface-imaging with nanometer-resolution by adding additional control-loops for real-time signal processing. This local information control-loop enables our nanorobot to automatically search for specific features and track them. Here, we present setup and performance of our current system prototype consisting of a 2D linear motor as sample stage and an AFM-like local probe.

I. INTRODUCTION

In the micro and nano world, visualization tools play a fundamental role in localizing targets and positioning miniaturized tools relative to them [1]. Traditionally, far-field optics such as light or electron microscopes are used to achieve this task. However, with such sensors alone, practical resolution and accuracy tends to be limited to several tens of nanometers. Electron microscopes may offer higher resolution but their use is restricted to vacuum environments. In contrast to far-field sensors, near-field probes typically operate in vacuum, ambient pressure, or fluid environments and offer nanometer-scale resolution, although with a much reduced field of view due to their proximity to the substrate.

In the (sub)micro world, the size of objects dictates the useful dimensions of sensors and actuators and generally necessitates integration of several sensing and/or actuation functions into a single pointed probe to gain full access to the small region of interest. Such sensors and actuators suitable for the nanometer world are already available from scanning probe microscopes [2]; however, autonomous nanorobots with overall dimensions in the sub-millimeter range are not yet feasible because of the size of current microprocessor technology and interface electronics. Therefore, today's scanning probe microscopes equipped with multifunctional sensors offer a good platform to implement and test concepts and control strategies for nanorobots.

In such a sensor-guided nanorobot, near-field probes are not primarily used in a microscope setup, i. e. to generate images, but rather as very sensitive and local tools to analyze and automatically follow user-specified nano-structures. To this end, we have developed strategies allowing the robot system to handle several different sensor inputs from a single multifunctional near-field probe [3] and to combine this information with global data and the user's a priori knowledge.

II. SETUP OF THE NANOROBOT

In our current nanorobot setup [4] we have chosen AFM tips as local sensors whose multifunctional characteristics allow us to measure different signals, e. g. topography or electrical potential, as well as to use them for nano-particle handling [5, 6, 7]. This sensor is mounted on a piezo tube scanner that applies scanning probe techniques to position the tip with nanometer precision. We extended this system with a coarse positioning device to enlarge the limited working area of the piezo scanner allowing the nanorobot to work on the whole surface of integrated circuits. In detail, we achieve a working range of 200 x 200 mm with a 2D linear stepping motor used for moving the sample's region of interest inside the piezo

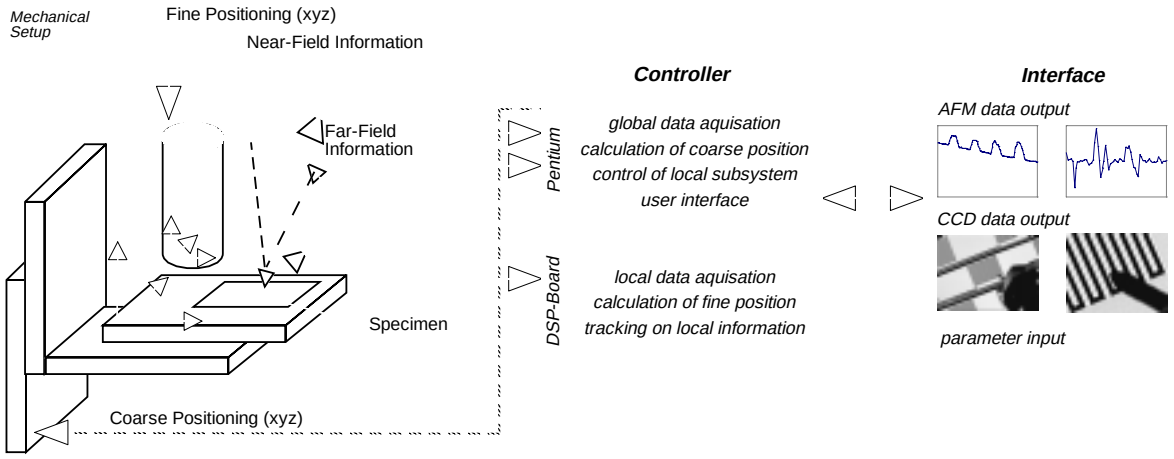

FIGURE 1: Setup of the nanorobot consisting of local and global sensors, actuators and controller including user interface.

tube's working space. Fig. 1 shows the basic setup which was complemented with several optical camera sensors to extend the tip's field of view and to provide wide-range observation of the specimen.

This mechanical system was further complemented by adding a controller consisting of a digital signal processor subsystem (DSP, Fulcrum DT3808, Data Translation) for local data processing and a standard personal computer (Pentium) for global data processing. The DSP subsystem is running independently of the host system under the real-time operating system SPOX allowing on-line acquisition and processing of near-field signals from the local sensor. The host system operates under Windows 95 enabling the far-field image processing as well as the data visualization for the graphical user interface to run in parallel tasks. Further, it provides a convenient interface that easily allows us to check local and global data as well as to interact with the robot system.

We implemented our first prototype of a sensor-guided nanorobot on a commercial atomic force microscope (AFM, Nanoscope IIIa, Digital Instruments, Santa Barbara). To this end, interfaces were added to the AFM controller for the position signals (in x, y, z), for sensor signals and for the mode switches governing the operating functions of the near-field probe, i. e. *tapping mode* for topography acquisition where the nanoprobe is oscillating in z-direction and only in brief contact with the substrate during each cycle, *lift mode* where the nanoprobe retraces the surface at a set distance above to perform non-contact measurements like electric potential mapping [3], and *approach* to bring the nanoprobe into the near-field of the substrate. Care was taken to design a modular system allowing us to use the AFM as a pure microscope with the Nanoscope controller alone or as a sensor-guided nanorobot together with the external controller.

III. Tracking of Local Signals

We implemented a tracking algorithm [11] capable of searching for microstructures with user-specified characteristics and following them under control of a vision system or user commands. Fig. 2 illustrates the flow chart of this tracking strategy. The user specifies the region of interest and the characteristics of the structure to be located and analyzed, e. g. its approximate width b, its height h_1 and h_2, the electrical potential, the slope a_1 and a_2, the signal level z_0, etc. The nanorobot then initiates a search procedure where data is acquired along extended line scans in the specified area and then compared with an analytical model of the desired structure, i. e. the shape of a circuit path and the potential over this path (Eq. 1) or an edge.

$$z(x) = \frac{h_1}{2}\tanh\left(2\frac{a_1}{h_1}\left(x+\frac{b}{2}\right)\right) + \frac{h_2}{2}\tanh\left(2\frac{a_2}{h_2}\left(x-\frac{b}{2}\right)\right) \ldots + 2z_0 + \frac{h_1-h_2}{2} \quad (1)$$

In detail, we calculate the correlation of the parameterized analytical shape z(x) and the line scan d(x) data for each signal class (i. e. topography, potential, amplitude error, etc.) (Eq. 2) and search for the maximum. According to the user's specification of the signal characteristics either the topography result only or both topography and potential are weighted and then transformed to a coordinate, which is the entrance point for the control loop.

$$c(x) = \sum_k z(x+k)d(x) \quad (2)$$

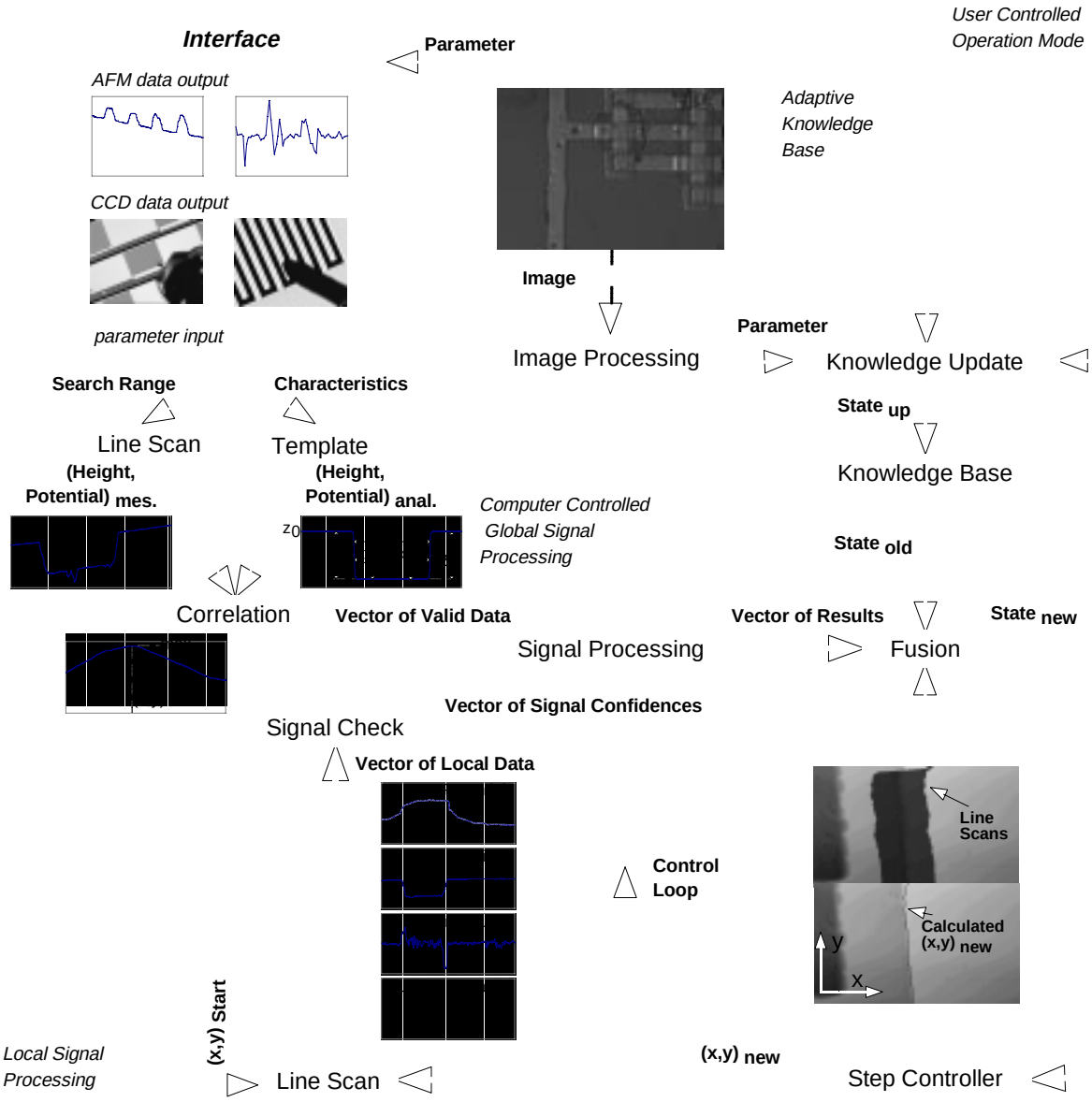

FIGURE 2: Schematic flow diagram for tracking user-specified features.

During tracking the multifunctional local sensor first acquires a vector of local data, i. e. the probe is moved to given interpolated positions between a start and an end point of a line and all signals of interest (i. e. topography, surface potential, amplitude error, etc.) are recorded at each point. Whereas sensitivity and noise of far-field sensors normally are smoothly varying functions with time, hence behave in a fairly predictable manner, near-field sensors like our AFM tips may exhibit large variations in performance since their signal transfer characteristics not only depend on the probe itself but also on the interaction with the substrate. For instance, loose adsorbates or dirt particles on the surface easily deteriorate resolution of the probe and increase signal noise. Therefore, the sensor data is first checked according to a priori knowledge, i. e. we weighted the amplitude error signal as less reliable than the topography or potential information due to its very strong dependence on noise and system parameters like feedback gains. Further, the signals are preprocessed to perform careful noise reduction and plane offset corrections which are necessary to improve the results of the following processing steps.

In our multifunctional sensor setup all channels are treated independently in the signal processing step where data is reduced and the necessary information extracted. We used different kinds of filters for each class of signals to calculate the necessary information.

For instance, the amplitude data is a control loop error signal in which an edge is represented by a sudden peak. We use minimum and maximum detectors combined with thresholding to extract this edge position.

In order to determine line and edge positions in topography signals several strategies are possible. One solution to detect edge positions is to search for low and high plateaus in the acquired data and locate the transition between them. Another strategy is to calculate the derivative [8] of the signal and search for minimum and maximum to find the steepest change and therefore the edge positions. Both solutions produce good results on well conditioned signals with little noise, but the fact, that the algorithms only take a few data points around the edge position into account, makes them strongly susceptive to noise in the signal and hence produce unreliable results for perturbed signals. That's why we implemented Canny [9, 10] filters to analyze the topography and potential signals. This class of filters calculates the convolution of the signal and an edge detector according to (Eq. 3) and performs edge detection and noise reduction in one step. The filter behavior can be controlled with the parameter s. Due to the fact that we use a convolution and therefore take the whole data line into account to calculate an edge position, the results depends little on signal noise and the filter produces much better results.

$$f(x) = -\frac{x\sqrt{e}}{s} e^{-\frac{x^2}{2s^2}} \qquad (3)$$

In the subsequent fusion step, all filter results (index j in Eq. 4 and 5) are merged into a single state according to the sensor confidence of each signal class. To this end, we treated each filter output as a statistical number $z_{i,j}$ with the calculated edge position as mean value. In order to weight this new position we assume that it is more reliable the closer it is located to the former edge position z_{i-1} calculated in the previous control cycle. Therefore, we set the deviation $\sigma_{i,j}$ proportional to the difference from the actual to the former edge location (Eq. 4). We then calculate the weighted sum (Eq. 5) of these probability numbers considering each signal's confidence $k_{i,j}$ determined in the signal check. In detail we balance the results with the signal confidence and the variance to the former edge position.

$$\sigma_{i,j} \propto \left| z_{i-1} - z_{i,j} \right| \qquad (4)$$

$$z_i = \sum_j k_{i,j} z_{i,j} \qquad (5)$$

Whereas a circuit path can be easily identified as a straight line with an optical microscope, within the limited field of view of the nanosensor there is an abundance of local curvatures or even imperfections. To facilitate tracking of such imperfect structures on the nanoscale we rely on a database in which we store the tracking parameters and accumulated information from previous control cycles. A strong connection of the knowledge base and the fusion step allows the nanorobot to weight the new state based on the stored parameters and the actual fused ones. Hence, we get stability of the system against noise and short-time break-downs of sensor signals with this dynamic knowledge base that can be updated with actual information from the local (AFM tip) as well as the global sensors (CCD cameras).

Therefore, this adaptive knowledge base also acts as an interface for overlaid tasks such as a vision sensor or user interactions. Finally the step controller transforms the new state calculated by the fusion process into the new position for the next control cycle.

The signal processing is complemented with an additional vision loop based on an optical microscope as a global sensor extracting information about the general topography of the circuit paths. With image processing algorithms additional information about the future circuit path trajectory are deduced and used to support the local sensor loop at critical situations like e. g. path intersections or branch outs. In addition, the user can also communicate with the system to enable the nanorobot to work in a semiautomatic mode under control of the operator. Both image processing and user are exchanging data via the interface of the knowledge base. In our current prototype we only use this interface in the semiautomatic mode and, therefore, the nanorobot only operates on local signals and user commands.

IV. Results: Nanorobot Performance

To evaluate the performance of our sensor-guided nanorobot, we used different microfabricated test structures. These devices exhibit a variety of characteristic surface structures on the micrometer and nanometer scale. We first show the tracking of rather big structures, namely microfabricated circuit paths with a width of 10 µm. Fig. 3a depicts the basic working strategy of our tracking algorithm. We first search for the structure in a starting phase and then track along the found path. During procedure 1 (Fig. 3b) the nanorobot is tracking the structure only according to local information without any further inputs from global sensors or the user. The algorithm is capable of compensating possible plane-offsets, changes in the sensor signal, and non-linearities due to the open-loop control of the piezo actuator, e. g. hysteresis, creep and drift effects. In pro-

cedure 2 the user interacts with the control loop to change the working direction at the 90° turn in the path. After this interaction, the local sensor control loop automatically follows the path again (procedure 3).

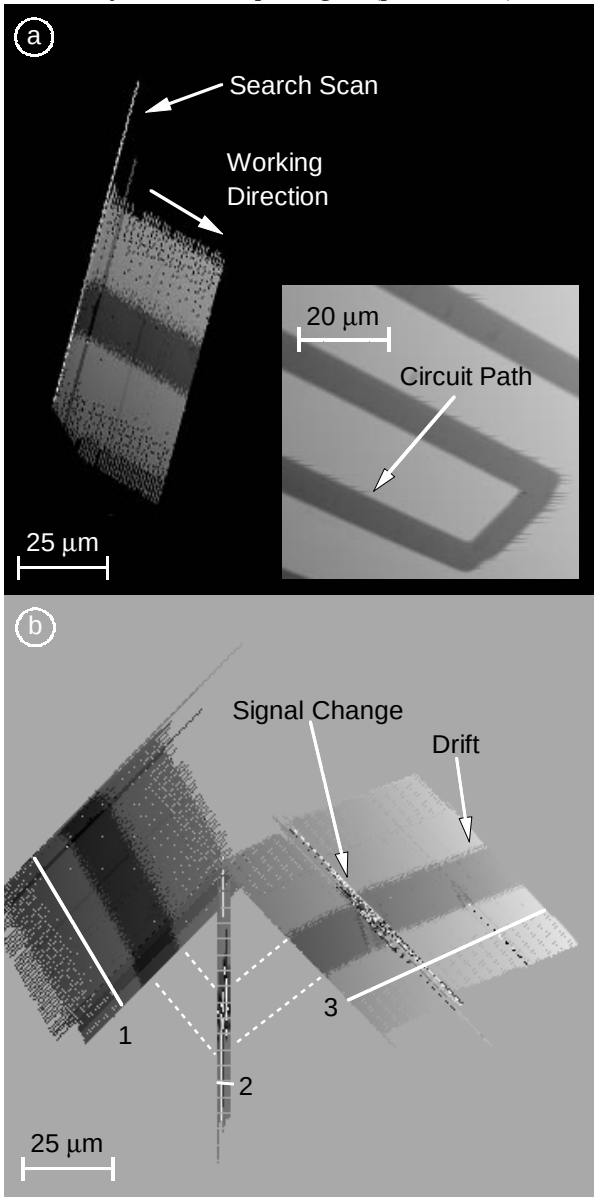

FIGURE 3: (a) Basic working principle of our nanorobot and overview of the sample structure. (c) Tracking with user interaction between procedure 1 and 2 as well as between procedure 2 and 3.

To evaluate the system's performance on the nanometer scale we used microfabricated test sample with 800 nm width circuit paths. Fig. 4 and 5 are displaying two of these structures. In Fig. 4b the nanorobot missed the correct starting position in the search scan and moved away. After hitting a circuit path the tracking algorithm follows it under control of the user who updates the scan angle of the nanorobot at each procedure change. In Fig. 5b we prove that the algorithm can automatically find and follow the path. Fig. 5c is showing the tracking task with changing of the step size by the user at less critical positions.

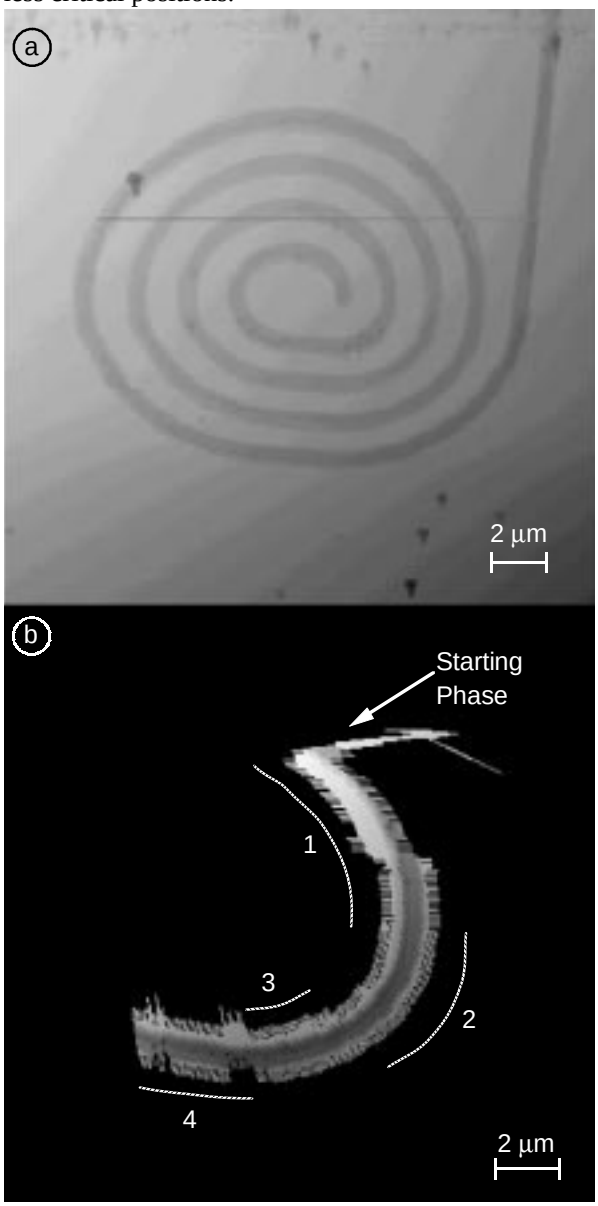

FIGURE 4: (a) Overview of swirl structure. (b) Tracking with user invention by changing the scanning angle between each procedure.

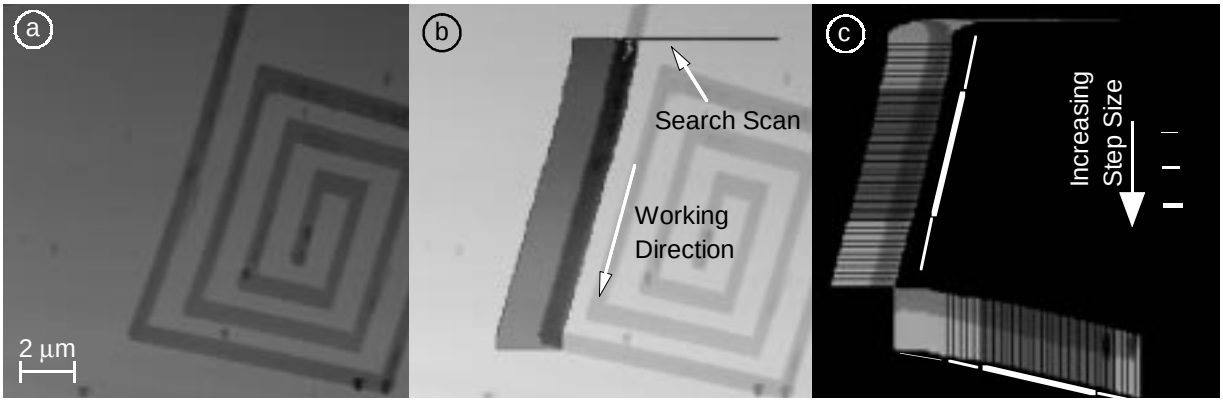

FIGURE 5: (a) Overview of microfabricated structure. (b) Search scan and tracking along a user-defined path. (c) Tracking with user interaction by changing forward step size and working direction at 90° turn.

V. OUTLOOK

In a next step we will implement the global sensor feedback to help the nanorobot in critical situations. Further we replace the Nanoscope AFM by our custom-made setup to extend the working range of the system. We also expect to implement a 2D position sensing device to correct the non-linearities of our piezo actuator with a closed-loop controller to improve the tip positioning accuracy.

We expect such a sensor-guided nanorobot to become a powerful and flexible tool for automated analysis of microfabricated devices, as well as repair of integrated circuits where critical functions depend on nanoscale structures.

VI. ACKNOWLEDGMENTS

We thank Heiko Jacobs and Serge Müller for their help with electric potential measurements using the Kelvin probe technique, Daniel Bächi for providing microfabricated test samples, as well as Dr. Helmut F. Knapp and Jan Frohn for critically reading this manuscript. This work was supported by the Swiss Federal Institute of Technology Zurich, Polyproject NANO II.

VII. REFERENCES

1. A. **Stemmer,** H. **Jacobs,** H. F. **Knapp,** *"Approaching the nanoworld,"* Proc. Microrobotics: Components and Applications, Boston, pp. 80-85, 1996
2. K. H.. **Wickramasinghe,** *"Scanning probe microscopy: current status and future trend,"* Journal of Vacuum Science and Technology A, vol. 8, pp. 363-368, 1990
3. H. O. **Jacobs,** H. F. **Knapp,** S. **Müller,** A. **Stemmer,** *"Potential measurement: a qualitative material contrast in SPM"*, Ultramicroscopy, vol. 69, pp. 39-49, 1997
4. A. **Stemmer,** M. **Brunner,** *"Sensor-guided nanorobots"*, SPIE Microrobotics and Microsystem Fabrication, Pittburgh, pp. 222-227, 1997
5. C. **Baur,** B. C. **Gazen,** B. **Koel,** T. R. **Ramachandran,** A. A. G. **Requicha,** L. **Zini,** *"Robotics nanomanipulation with an SPM in a networked computing environment"*, J. Vacuum Sc. & Tech. B, Vol. 15, No. 4, pp. 1577-1580, 1997
6. A. A. G. **Requicha,** *"Nanorobotics"*, Handbook of Robotics, New York: John Wiley & Sons, to appear, available at http://lipari.usc.edu/~lmr/html/publications.html
7. A. A. G. **Requicha**, C. **Baur**, A. **Bugacov**, B. C. **Gazen**, B. Koel, A. **Madhukar**, T. R. **Ramachandran**, R. **Resch** and P. **Will**, "*Nanorobotic assembly of two-dimensional structures*", Proc. IEEE Int'l Conf. on Robotics & Automation, Leuven, pp. 3368-3374, 1998.
8. R. C. **Gonzalez,** R. E.. **Woods,** *"Digital image processing"*, Addison-Wesley, 1993
9. J. **Canny,** *"A computational approach to edge detection"*, IEEE Transactions on Pattern Analysis and Machine Intelligence, vol. 8, pp. 679-698, 1986
10. V. S. **Nalwa,** T. O. **Binford,** *"On detection edges"*, IEEE Transactions on Pattern Analysis and Machine Intelligence, vol. 8, pp. 699-714, 1986
11. D. W. **Pohl,** R. **Möller,** *" "Tracking" tunneling microscopy"*, review of Scientific Instruments, vol. 59, pp 840-842, 1998